Accepted Manuscript

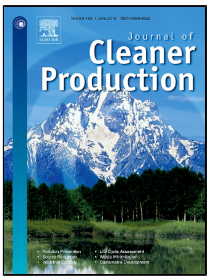

Efficient removal of arsenate from oxic contaminated water by colloidal humic acid-coated goethite: batch and column experiments

Daniela Montalvo, Ruth Vanderschueren, Andreas Fritzsche, Rainer U. Meckenstock, Erik Smolders

PII:	S0959-6526(18)31074-6
DOI:	10.1016/j.jclepro.2018.04.055
Reference:	JCLP 12636
To appear in:	*Journal of Cleaner Production*
Received Date:	24 October 2017
Revised Date:	05 April 2018
Accepted Date:	06 April 2018

Please cite this article as: Daniela Montalvo, Ruth Vanderschueren, Andreas Fritzsche, Rainer U. Meckenstock, Erik Smolders, Efficient removal of arsenate from oxic contaminated water by colloidal humic acid-coated goethite: batch and column experiments, *Journal of Cleaner Production* (2018), doi: 10.1016/j.jclepro.2018.04.055

Word count:7572

Efficient removal of arsenate from oxic contaminated water by colloidal humic acid-coated goethite: batch and column experiments

Daniela Montalvo*[1], Ruth Vanderschueren[1], Andreas Fritzsche[2], Rainer U. Meckenstock[3], and Erik Smolders[1]

[1]Division of Soil and Water Management, KU Leuven, Kasteelpark Arenberg, Heverlee, Belgium

[2] Institut für Geowissenschaften, Friedrich-Schiller-Universität Jena, D-07749 Jena, Germany

[3] Biofilm Centre, University Duisburg-Essen, 45141 Essen, Germany

*Corresponding author E-mail address: daniela.montalvogrijalva@kuleuven.be

Abstract

Arsenic (As) contamination of groundwater frequently occurs and there is a need for cost-effective *in situ* remediation techniques. The injection of iron oxide colloids coated with humic substances has been proposed. This technology is based on injecting mobile humic acid-coated goethite colloids that are subsequently deposited by aggregation in the contaminated zone where the ionic strength is large, thereby creating an *in situ* reactive barrier for As. While coagulation and deposition are desirable for colloid immobilization, its effect on adsorption properties have been previously overlooked. This study was set up to investigate if i) humic acid-coated goethite colloids retain their As(V) adsorption properties after coagulation in quartz sand and ii) if batch As(V) adsorption data can predict As immobilization in columns at variable flow conditions. Equilibrium batch adsorption experiments showed that humic acid-coated goethite colloids coagulated and deposited on quartz sand have equal As(V) adsorption capacity, but two-fold lower affinity than humic acid-goethite colloids in suspension. This results indicated that there were some interactions between the sand and colloids but the overall adsorption capacity was not affected. Column experiments using sand coated with humic acid-goethite colloids (2.80 mg goethite g^{-1} sand) and stepwise injection of As(V) (1 4.9 mg As L^{-1}) showed a highly efficient As(V) removal from the liquid phase as the outflow As(V) concentrations remained below the drinking water limit (10 µg As L^{-1}) until about 45% of the sorbent capacity (30 mg As g^{-1} goethite) was reached. The flow rate dependent leachate As concentrations, including responses to stop-flow events, illustrated non-equilibrium sorption. The equilibrium batch adsorption

parameters failed to predict the observed As(V) breakthrough curves, which were better fitted with a chemical non-equilibrium consideration. This study confirms the feasibility of the technology on lab-scale but suggests that safety factors must be embedded to account for As(V) by-pass flow that could occur during field applications.

Keywords

iron oxide colloids, humic acids, reactive barrier, arsenic adsorption, transport, coagulation

1. Introduction

Arsenic (As) contamination of groundwater poses serious threat to the environment and human health through use as drinking and irrigation water (Smedley and Kinniburgh, 2002). It has been estimated that over 226 million people worldwide are exposed to As via the intake of contaminated water and food (Murcott, 2012). Due to the high toxic nature of As and the well documented negative health effects associated to its chronic exposure, the World Health Organization (WHO) set a limit concentration of 10 μg L^{-1} for As in drinking water (WHO, 2011). This standard has been adopted in the legislation of many countries; however, in many places the previous WHO limit of 50 μg L^{-1} is still in place mainly due to technical difficulties and the lack of an effective remediation technology (Cundy et al., 2008).

Background As concentrations in natural water are mostly below the WHO guideline value; however, elevated concentrations (> 5000 μg L^{-1}) have been reported in groundwater linked to geogenic sources or anthropogenic activities (Smedley and Kinniburgh, 2002). In aquatic environment the predominant forms of As are the inorganic species arsenite As(III) and arsenate As(V). At circumneutral pH, As(V) as ($H_2AsO_4^{-1}$ and $HAsO^{-2}$) is the most stable form of As in oxic water; whereas As(III) as ($H_3AsO_3^0$) is more prevalent in anoxic water (Mohan and Pittman, 2007). Arsenite is more mobile and toxic than arsenate and both species have strong affinity for iron oxides (*e.g.* ferrihydrite, goethite, hematite) (Dixit and Hering, 2003), also under natural conditions, where several competitors for association with iron oxides coexist (Fritzsche et al., 2011). Hence, the use of iron oxides to adsorb and remove As from groundwater have been widely investigated for remediation of contaminated sites (Mohan and Pittman, 2007).

In recent years, nanoremediation has been proposed as a potential more cost effective technology for *in situ* remediation of soil and groundwater (Karn et al., 2009). Nanoremediation entails the use of colloidal particles, which are defined as material with at least one dimension between 1 1000 nm (Christian et al., 2008). The large surface area and, hence, high adsorption capacity make colloidal size particles very attractive for remediation purposes compared to non-colloidal macro size aggregates. Additionally, small particles have better mobility and can achieve a wider radius of influence after injection in the subsurface. In this context, engineered goethite (α-FeOOH) colloids, which have a very high affinity for As(V), combine all desirable characteristics for *in situ* remediation of As contaminated groundwater.

The application of goethite (Goe) colloids for *in situ* remediation of contaminated groundwater consists of the injection of a suspension of colloids into the contaminated plume and then deposition *in situ* by coagulation (*e.g.* particle aggregation) in the porous matrix of the aquifer material due to the conditions of groundwater (high ionic strength, pH) (Tosco et al., 2014). In this way, the colloidal Goe forms a *reactive zone* within the aquifer through which contaminated water is filtered and decontaminated. The immobilization of the Goe colloids after their injection into the aquifer is mandatory to prevent the export of Goe from the reactive zone; however, coagulation may affect its sorption properties. Coagulation can reduce the Goe reactive surface area and thus the adsorption properties for contaminants (Hotze et al., 2010). While there has been substantial research on the adsorption of As onto iron oxide minerals (Aredes et al., 2012; Mamindy-Pajany et al., 2011) and iron-coated sand (Benjamin et al., 1996; Mähler and Persson, 2013) there are, to the best of our knowledge, no studies that investigate the effect of aggregation and deposition of colloidal iron oxides onto a substratum on their adsorption capacity of contaminants. This information is mandatory prior to field applications and thus the relevance of this study.

A second aspect that needs investigation is to what extent the deposited particles form a homogenous reactive barrier for instantaneous reaction with the contaminants. This translates to the question if the reactive transport of the contaminant can be modelled assuming local equilibrium *i.e.* if the resident solution concentration is locally at equilibrium with the adsorbed concentration. In soils, the local equilibrium assumption (LEA) for the transport of As is mostly violated, resulting in breakthrough curves featuring early breakthrough and distinct tailing (Darland and Inskeep, 1997). Non-equilibrium transport of As has been observed in studies that were conducted at large (32 cm h^{-1}) (Williams et al., 2003) or low (0.34 cm h^{-1}) (Zhang and Selim, 2006) pore water velocities. For colloidal Goe deposition, it is possible that homogenous thin layers of particles may yield a large contact area between the mobile water and the sorbent, suggesting that the LEA may apply to a greater extent.

Against this background, a laboratory study was set up to investigate the feasibility of applying Goe colloids as an adsorbent for the removal of As(V) in an aquifer. Previously, humic acid-coated goethite (HA-Goe) colloids were synthesized showing sufficient colloidal stability in water for subsurface injection. For these HA-Goe colloids, studies were set up to address both questions described above, *i.e.* i) if the colloids retain their efficient As(V) adsorption properties after deposition on an aquifer model substrate and ii) if the LEA is valid during reactive transport. The column study addresses the question to what extent the WHO drinking water limit can be met after passage of As-spiked solutions through a reactive zone,

where HA-Goe is present. It is hypothesized that there will be a reduction in As adsorption capacity due to the aggregation and deposition of the HA-Goe colloids but that, overall, the LEA during reactive transport is met. First, a range of batch As adsorption experiments with colloidal HA-Goe and non-colloidal HA-Goe, which was deposited onto quartz sand, were conducted. Second, a suite of column experiments were conducted at different As(V) concentrations and different flow rates to determine its effects on the capacity and efficiency of the reactive barrier for the removal of As(V). Additionally, flow interruption events were included to gain better insights into possible kinetic limitations during the transport of As(V). The LEA was tested by forward modelling the column data with the convection-dispersion equation (CDE) using parameter values independently obtained from batch equilibrium adsorption. This study did not address the adsorption of As(III) under anoxic conditions since iron(III) oxides are not stable under such conditions, *i.e.* this study is addressing the potential to remediate oxic groundwater.

2. Materials and Methods

2.1. Humic acid-coated goethite colloids

A stock suspension of goethite colloids coated with humic acids (HA-Goe) [66.4 g iron (Fe) L^{-1}; 11.2 g organic carbon (OC) L^{-1}] was synthesized according to US patent 8921091B2 (Meckenstock and Bosch, 2014) and provided by the University of Duisburg-Essen.

Analysis with X-ray diffraction (XRD) and fourier-transform infrared (FTIR) spectroscopy revealed that the desired HA-Goe colloids were obtained from synthesis (Figure 1A, B). The presence of humic acids (HA) was revealed by carboxyl-induced bands (Socrates, 2004), which are commonly observed in mineral-associated natural organic matter (Kleber et al., 2015) and by the negative net-surface charge of the HA-Goe colloids at pH 7.3 (Zeta potential -37 ± 4 mV), where goethite exhibits a net-positive surface charge (Kosmulski, 2009). The observed traces of kaolinite were introduced due to impurities in HA (Figure 1B; molar ratio goethite:kaolinite 283:1). Generally, HA-Goe used in this study had a rather low long-range order compared to goethite that is commonly synthesized in the laboratory. This was indicated by comparably broad reflexes in the diffractogram. This points to comparably small-sized crystallites in HA-Goe, which was supported by a high specific surface area (202.4 ± 0.3 m^2 g^{-1}; mean ± min/max deviation from duplicate analysis) and by the corresponding scanning electron microscopy (SEM) images (Figure 1D, E). The latter showed nano-sized needles, which were assembled in aggregates of different size. The offset in hydrodynamic diameters determined with dynamic light scattering (DLS; intensity-

weighted; 243 ± 125 nm) and nanoparticle tracking analysis (NTA; number-weighted; 186 ± 69 nm; Figure 1C) indicate that the HA-Goe suspension contained colloids with a broad size distribution, while the number of smaller colloids (<200 nm) exceeded the number of larger colloids (>200 nm).

Unless otherwise indicated, the stock of HA-Goe colloids used in this study was diluted with Milli-Q water (18.2 MΩ cm^{-1}) to the desired working concentration to perform the experiments.

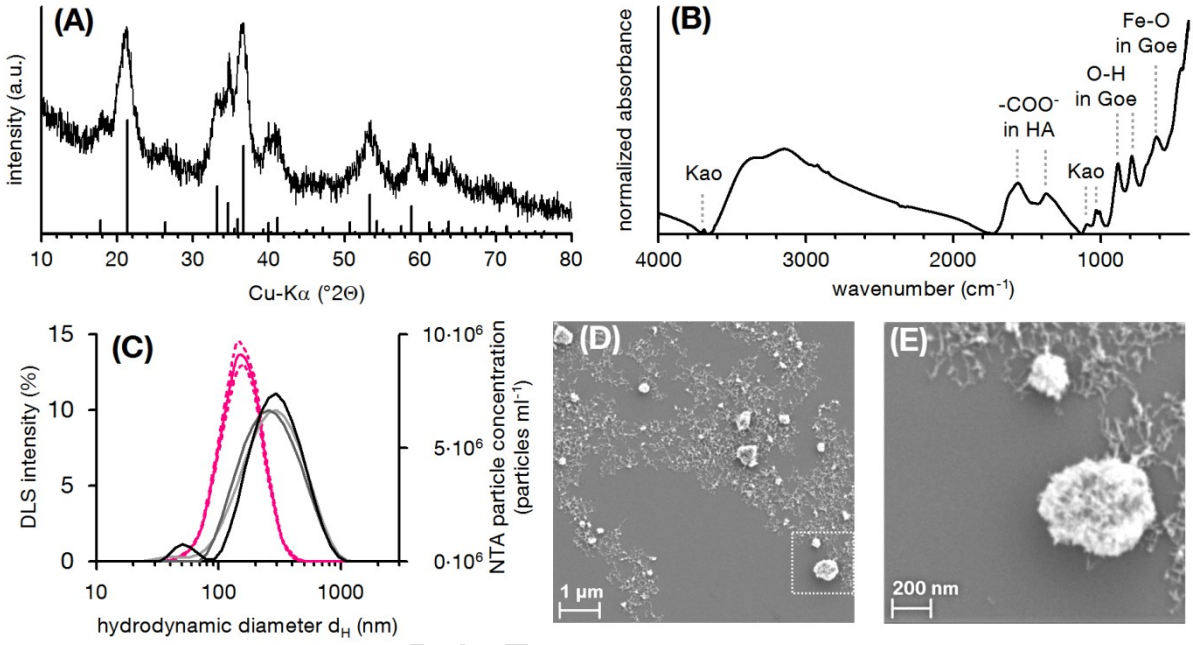

Figure 1 Characterization of the initial humic acid-coated goethite (HA-Goe) colloids before exposition to 5 mM Ca^{2+} and/or deposition on quartz sand. (A) Powder X-ray diffractogram, (B) Fourier-transform infrared spectrum, (C) hydrodynamic diameter distributions as estimated with dynamic light scattering (DLS) analysis (triplicate; black/grey graphs) and nanoparticle tracking analysis (NTA; quintuplicate, solid pink graph: mean, dashed pink graphs: standard deviation), and (D,E) scanning electron images. (E) = region marked in (D). Bars in (A): goethite (Downs and Hall-Wallace, 2003). Kao: kaolinite, HA: humic acid, Goe: goethite.

2.2. Sand coated with humic acid-goethite colloids

Sand coated with humic acid-goethite colloids (HA-Goe-coated sand) was prepared by optimizing a procedure that favors the deposition of HA-Goe colloids on the substrate by adjusting the pH and ionic strength of the colloidal suspension (Scheidegger et al., 1993). As previously indicated, it was hypothesized that the as prepared HA-Goe-coated sand may have a much lower adsorption capacity compared to the HA-Goe colloids in suspension, since the reactive sites from deposited colloids may be hindered and not readily accessible for

adsorption. To prepare HA-Goe-coated sand, acid washed sand [Dorsilit 8, grain size 0.3 0.8 mm, silica (SiO_2) 97.9% by weight, 23 ± 4 µg Fe g^{-1} sand] was mixed with 10 g L^{-1} of HA-Goe colloidal suspension diluted in 10 mM calcium chloride ($CaCl_2$) at pH 7. The high calcium (Ca^{2+}) concentration is likely the main factor causing aggregation by reducing the negative potential at the humic acid coated surface through adsorption and/or forming Ca bridges (Philippe and Schaumann, 2014). After the sand had settled, the supernatant suspension was removed and the HA-Goe-coated sand was dried at room temperature. The Fe content of the HA-Goe-coated sand (1.37 ± 0.10 mg Fe g^{-1} sand) was determined by inductively coupled plasma optical emission spectrometry (ICP-OES, Thermo Scientific ICAP 7400 Duo) after extraction with *aqua regia* [hydrochloric acid (HCl):nitric acid (HNO_3)1:3]. This Fe concentration is equivalent to 2.80 ± 0.2 mg HA-Goe g^{-1} sand.

2.3. Batch adsorption experiments

Adsorption isotherms were conducted at different pH (5.5 7.5) to determine the effect of pH on the capacity of HA-Goe colloids to adsorb As(V). The pH values selected for batch adsorption experiments are within the range for groundwater in natural conditions (Ayotte et al., 2011). Batch experiments were carried out at a constant temperature of 20°C and in 50 mL polypropylene tubes. Aliquots of the HA-Goe suspension (4 mL, 0.7 g goethite L^{-1}) were placed into a dialysis membrane for phase separation (Spectra/Por 4, 12-14 kDa cutoff) and equilibrated with 20 mL of sodium arsenate ($Na_2HAsO_4 \cdot 7H_2O$) solution of increasing As concentrations ranging from 0 to 100 µM. The contact solutions also contained 5 mM $CaCl_2$ as background electrolyte and 5 mM of either 2-(N-morpholino)ethanesulfonic acid (MES buffer, pH 5.5 and 6.5) or 3-(N-morpholino)propanesulfonic acid (MOPS buffer, pH 7.5) to maintain constant pH. Preliminary tests showed that there was no influence of these buffers on the adsorption of As(V) in the experimental conditions used. The HA-Goe suspensions were shaken for 72 h on an end-over-end shaker. Thereafter, a subsample of the contact solution was acidified (2% HNO_3) and the concentration of As in the solutions was determined by ICP-OES (189 nm wavelength). The detection limit (DL) of the ICP-OES for As is 1 µg L^{-1} and preliminary comparison of the As solutions between inductively coupled plasma mass spectrometry (ICP-MS; DL 0.05 µg L^{-1}) and ICP-OES showed excellent agreement in the 5 50 µg As L^{-1} range. The concentration of adsorbed As(V) was calculated by subtracting the equilibrium solution concentration from the measured total initial concentrations. All chemicals used in the experiments were of analytical grade and solutions were prepared with Milli-Q water (18.2 MΩ cm^{-1}). The same procedure was adopted for

As(V) adsorbed onto HA-Goe-coated sand. For the adsorption experiments, 2 g of HA-Goe-coated sand was placed into a dialysis membrane (12-14 kDa) and equilibrated for 72 h with solutions containing increasing concentrations of As(V) 0-100 µM, 5 mM $CaCl_2$ and 5 mM MOPS, pH 7.5. The Ha-Goe-coated sand was placed in dialysis membranes to have the same experimental conditions as in the batch experiments with colloidal HA-Goe aggregates. Additionally, a blank sand (Dorsilit 8, quartz sand uncoated) *i.e*. sand without HA-Goe deposited colloids was included, and the As(V) adsorption data were corrected for sorption to this uncoated sand to obtain As(V) adsorbed to the HA-Goe aggregates. All adsorption experiments were conducted in duplicates.

2.4. Column experiments

Column experiments were conducted to evaluate the adsorption of As(V) onto HA-Goe-coated sand at two inlet concentrations and three Darcy velocities 0.12, 0.3 and 1.5 cm h^{-1}. The column experiments (10 columns in total) were run in duplicates for each of three flow rates and two concentrations. Except for the low As(V) concentration where only two flow rates were included (1.5 and 0.3 cm h^{-1}). Glass columns of 2 cm internal diameter and 12 cm length were packed with 51 g of acid washed sand (Dorsilit 8) of which 15 g corresponded to a layer of HA-Goe-coated sand which was located in the middle part of the column. Columns were wet-packed to avoid air entrapment and were fitted with end-caps that contained *o*-rings for sealing and fritted glass filters (P0, pore size 160 250 µm) to facilitate the uniform distribution of the influent solution and prevent any loss of sand during the experiment. The columns were leached bottom-up with a background solution containing 5 mM $CaCl_2$ and 2 mM MOPS pH 7.5 for several pore volumes (PV) to equilibrate the system. Solutions of As(V) (low concentration: 1.01 ± 0.01 mg L^{-1} or high concentration: 4.58 ± 0.08 and 4.91 ± 0.10 mg L^{-1}) were injected for 57 149 PV until the effluent concentration was approximately 95% of the inlet concentration, which indicated the HA-Goe-coated sand was nearly saturated with As(V). Thereafter, the columns were flushed with the background solution [without As(V)] until the outflow concentrations were close to baseline. Effluent samples were collected periodically and the concentration of As(V) was determined by ICP-OES after acidification with 2% HNO_3. Iron was also measured in the effluents and the concentrations were lower than the limit of detection (0.3 µg Fe L^{-1}), which indicated no mobilization of goethite during the experiments. During the injection of As(V), the flow was interrupted

completely for 24 h to evaluate the effect of extended liquid-solid contact times on the transport of As(V).

The transport of bromide (Br^-), which was added as inert tracer, was also conducted to obtain physical transport parameters and to evaluate if physical non-equilibrium conditions (*i.e.* immobile water region) existed inside the columns. A pulse of 0.6 pore volumes (PV) of 1 mM Br^- was injected and the effluent samples were analyzed by ion chromatography (Dionex ICS-2000 with AS17-C columns).

3. Results and Discussion

3.1 Arsenate adsorption to humic acid-coated goethite colloids

Adsorption isotherms at pH 5.5, 6.5 and 7.5 were conducted to evaluate the effect of pH on the adsorption of As(V) onto HA-Goe colloids. The adsorption data (Figure 2) exhibited the feature of a Langmuir isotherm, formally indicated by:

$$q = \frac{b \cdot KL \cdot ceq}{1 + KL \cdot ceq} \qquad \text{Eq. 1}$$

where, q is the amount of As(V) adsorbed per gram of HA-Goe (mg g^{-1}), c_{eq} denotes the equilibrium concentration of the As(V) in solution (mg L^{-1}), K_L is the Langmuir constant (L mg^{-1}) that relates the affinity of binding sites and b is the adsorption capacity (mg g^{-1}). The adsorption of As(V) was not significantly ($p > 0.05$ level) affected by the pH of the solution (Figure 2). Different from other oxyanions (*e.g.* phosphate), adsorption of As(V) onto goethite has been shown to be less dependent on pH and ionic strength (Antelo et al., 2005). Studies that reported an effect of pH indicated that As(V) adsorption onto goethite generally decreases with increasing pH, particularly at pH above 7 and this effect is more pronounced at high As loading (Dixit and Hering, 2003).

In the present study, a relatively high concentration of Ca^{2+} (5 mM) as background electrolyte was used in the adsorption experiments in order to mimic that of contaminated groundwater. The goethite colloids used in this study were coated with humic acids in order to enhance colloidal stability and hence are negatively charged (Zeta potential -37 mV at pH 7.3). It is well accepted that functional groups of humic/fulvic substances are prone to form complexes with divalent cations (*e.g.* Ca^{2+}) (Weng et al., 2005). Therefore, it is likely that the presence of Ca^{2+} ions may have masked the effect of pH, as Ca^{2+} can enhance the adsorption of As(V) onto iron oxides by increasing the positive charge near the negatively charged surfaces (Antelo et al., 2015).

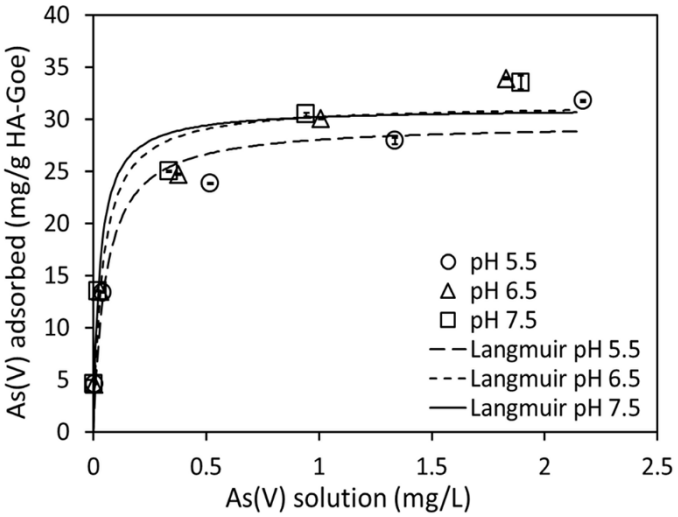

Figure 2 Adsorption isotherms of As(V) onto humic acid-coated goethite (HA-Goe) colloids at variable pH. Background electrolyte 5 mM $CaCl_2$ and 5 mM MES or MOPS. Symbols represent experimental results and dotted lines the fitted Langmuir model. Standard errors from duplicate treatments are smaller than the size of the symbols.

The adsorption capacities calculated from the Langmuir equation were unaffected by the pH values (t-test, $p > 0.05$ level) and were, on average, 31 mg As g^{-1} HA-Goe (Table 1). Values of sorption maxima for goethite reported in literature vary greatly (0.45 61 mg As(V) g^{-1} goethite) and direct comparisons are difficult due to the different experimental conditions. For instance, Wu et al., (2014) measured an adsorption maxima of 61 mg As g^{-1} at pH 7 for goethite nanoparticles that have a specific surface area of 293 m^2 g^{-1}. From the adsorption isotherm data by Antelo et al., (2005) an adsorption maxima of 11 mg As g^{-1} was estimated at pH 7 for goethite material with a surface area of 71 m^2 g^{-1}. Much lower adsorption capacities (0.45 mg As g^{-1} goethite) have been reported in natural iron oxides of lower surface area (2 m^2 g^{-1}) (Giménez et al., 2007). Over all, the adsorption maxima calculated for HA-Goe used in this study is high considering that the colloids were stabilized with humic acids which can decrease As(V) adsorption via electrostatic repulsion or by occupying the reactive surface sites (Weng et al., 2009). Recently, Otero-Fariña et al., (2017) investigated the adsorption of As(V) onto bare goethite and goethite coated with humic acids containing different proportions of carbon (2 8%). They found a decrease in the goethite reactive surface area from 100 m^2 g^{-1} (bare goethite) to about 60 m^2 g^{-1} (humic acids coated goethite containing about 8% C). This decrease in reactive surface area was evidenced also by a 25 to 40% reduction in the amount of As(V) adsorbed onto goethite containing 4 or 7% C. Similarly,

humic substances negatively affected the efficiency of granular ferric oxide to remove As(V) from aqueous solutions as reported by Saldaña-Robles et al., (2017).

3.2 Arsenate adsorption to humic acid-coated goethite colloids immobilized in quartz sand

The adsorption isotherm of the uncoated sand (blank sand) was nonlinear and could be described by the Langmuir model. The capacity (*b*) of uncoated sand to remove As(V) from solution was clearly lower than that of HA-Goe-coated sand (25 µg As g^{-1} uncoated sand vs. 114 µg As g^{-1} coated sand), which corroborated its main function as supportive material for the HA-Goe aggregates (Figure 3).

The comparison of As(V) adsorption onto the surface of HA-Goe-coated sand at pH 7.5 versus that onto the original HA-Goe colloids is shown in Figure 3.

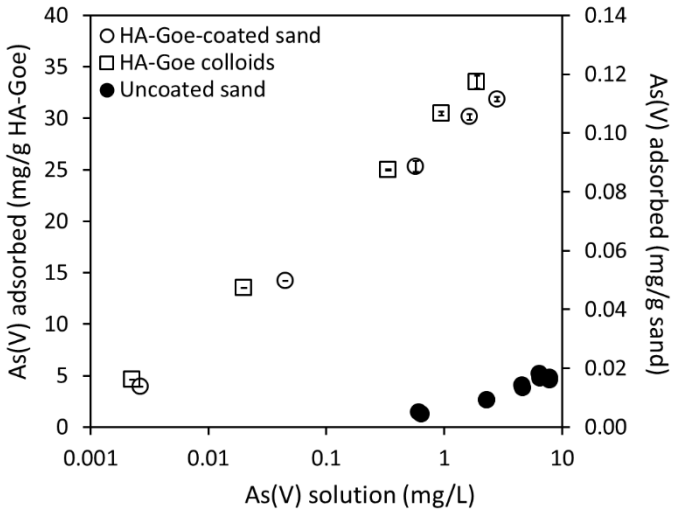

Figure 3 Semi-log plot of the adsorption isotherm of As(V) onto humic acid-coated goethite (HA-Goe) colloids in suspension, HA-Goe-coated sand and uncoated sand at pH 7.5. Background electrolyte 5 mM $CaCl_2$ and 5 mM MOPS. The standard errors are smaller than the size of the symbols.

The adsorption capacities *b* for As(V) estimated from fitting the Langmuir model were not significantly different ($p > 0.05$) between the HA-Goe-coated sand and the colloidal HA-Goe with *b* values of 31 and 30 mg As g^{-1} goethite (Table 1). However, the K_L parameter of the Langmuir equation that reflects the affinity of sorbate to the sorbent was two times larger for colloidal HA-Goethite compared to that of HA-Goe-coated sand. These results indicate that there was a more favorable adsorption (*i.e.* stronger adsorption affinity) of As(V) to colloids in suspension than to those coated on sand particularly, at low As(V) loading. Note that both adsorption experiments have used an equally high concentration of Ca^{2+} (5 mM) to allow comparison of As adsorption in equal, and relevant ionic scenarios. At this concentration of

316 Ca^{2+}, aggregation and sedimentation of the HA-Goe colloids was visible during the
317 experiment. A subsample of the HA-Goe colloidal suspension that was exposed to the contact
318 solution was taken and the hydrodynamic diameter measured by DLS (>1000 nm) was well
319 above the size of the original suspension (Figure 1C). Calcium concentrations of 1 mM are
320 sufficient to cause aggregation of such particles (Bollyn et al., 2016). This means that the
321 HA-Goe colloidal suspension as used might contain non-colloidal aggregates with lower As
322 adsorption affinity/capacity than the original suspension which was also low in Ca and
323 sodium (Na) dominated.
324
325 Table 1 Estimated Langmuir parameters *b* and K_L and corresponding best fit standard error
326 for the adsorption of As(V) onto humic acids coated-goethite (HA-Goe) colloids and HA-
327 Goe-coated sand. The K_L of the original particles at pH 7.5 is significantly (*, $p < 0.05$, t-test)
328 above that of the coated sand indicating a loss of As affinity of the particles once coated to
329 sand.

Adsorbant	Langmuir parameters	
	b (mg As(V) g^{-1} HA-goethite)	K_L (L mg^{-1})
HA-Goe colloids		
pH 5.5	29.6±1.06	18.2±3.91
pH 6.5	31.5±1.33	24.2±6.42
pH 7.5	30.9±1.23	37.6±9.69*
HA-Goe-coated sand		
pH 7.5	30.6±1.03	18.9±4.10

330
331 3.3 Transport of As(V) in columns containing humic acid-goethite coated sand
332 The Br^- breakthrough curves were fitted to the one-dimensional CDE (one fit per replicate
333 column) to obtain the parameters pore water velocity (*v*) and dispersion coefficient (D)
334 (Šimůnek et al., 1999) that are shown in Table 2. Bromide breakthrough curves were
335 symmetrical, exhibited no tailing and were well described by the CDE that is based on LEA
336 (r^2 = 0.993-0.998). The optimized dispersion coefficient parameters increased linearly with
337 increasing pore water velocity but the longitudinal dispersivity (λ) calculated by the ratio
338 between D and *v* did not differ greatly. Given that the transport of Br^- was well predicted by
339 the equilibrium model it was assumed that physical non-equilibrium was negligible in the
340 columns (Brusseau et al., 1989). The average effective porosity estimated from the Br^- tracer
341 tests was 0.40 ± 0.01. The λ values calculated from D and *v* parameters were subsequently
342 used to predict As(V) transport based on the CDE model using HYDRUS-1D.
343

Table 2 Estimates of the transport parameters dispersion coefficient (D) and pore water velocity (*v*) for the convection-dispersion model (CDE) obtained by least-square fit with STANMOD. Values in parenthesis are corresponding standard deviations of the two column replicates.

Darcy velocity	D	*v*	λ§	r^2
cm h^{-1}	cm^2 h^{-1}	cm h^{-1}	cm	
1.5	0.21 (0.01)	3.75 (0.13)	0.06 ± 0.004	0.998
0.3	0.05 (0.003)	0.78 (0.001)	0.06 ± 0.004	0.995
0.1	0.02 (0.002)	0.36 (0.002)	0.07 ± 0.007	0.993

§Dispersivity, λ=D/*v*

Column transport experiments were conducted to evaluate the efficiency of HA-Goe in removing As(V) from contaminated water. Since the results from batch experiments indicated some adsorption of As(V) onto uncoated sand, additional blank sand columns were included to understand the transport of As(V) in this system (data not shown). The breakthrough curves of As(V) in the HA-Goe free (blank) columns were fitted to the nonlinear equilibrium adsorption model of HYDRUS resulting in *b* of 2.49 mg As kg^{-1} sand and K_L of 0.15 L mg^{-1}, and which corresponded to a retardation coefficient of 1.41.

For the column studies, a layer of HA-Goe-coated sand was used to mimic the reactive barrier after the injection of the HA-Goe colloids in the subsurface. The breakthrough curves of As(V) at three pore water velocities (3.75, 0.78, 0.36 cm h^{-1}) and initial As(V) concentration of 4.6 4.9 mg L^{-1} are shown in Figure 4. All breakthrough curves were asymmetric with a relatively sharp front after about 14 17 PV and exhibited tailing. The As(V) breakthrough was considered as complete when the concentration of As in the leachate was 95% to that of the inlet concentration (C/C_0 = 0.95). The adsorption maxima calculated from the integration of the breakthrough curves was 34.1, 26.4 and 16.2 mg As g^{-1} HA-Goe, for columns at 0.36, 0.78 and 3.75 cm h^{-1} pore water velocities, respectively. This means that the highest adsorption capacity was observed in the columns with the lowest flow rate, which can be explained by the longer contact time of As(V) with HA-Goe-coated sand. The residence times of water in the columns are, depending on flow rates, between 3 and 33 h, and are relatively short considering that in the batch experiments samples were equilibrated for 72 h. The total amount of As(V) adsorbed at the lowest velocity (34 mg As g^{-1} HA-Goe) is close to the value calculated from the equilibrium batch adsorption experiments (30 mg As g^{-1} HA-Goe).

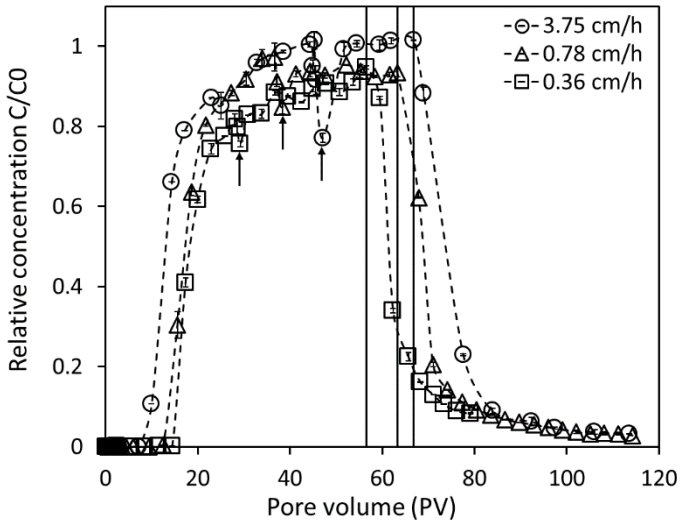

Figure 4 Breakthrough curves for As(V) at three pore water velocities (0.36, 0.78 and 3.75 cm h^{-1}) and As inlet concentration 4.6 4.9 mg L^{-1}. Arrows denote flow interruption and solid vertical lines indicate the points when the influent As(V) concentration was reduced to zero.

The effect of pore water velocity on the transport of As(V) was observed by a leftward shift of the breakthrough curves (earlier breakthrough) with increasing pore water velocity. In addition, it was calculated the fraction of previously loaded As(V) that was not recovered in the leachates in the period after the influent concentration decreased to zero. That non-recovered fraction was 31.5, 21.5 and 14% for columns at pore water velocities 0.36, 0.78 and 3.75 cm h^{-1}, suggesting that longer residence time allowed stronger As immobilization. Similar velocity effects on sorption and transport of As(V) have been previously reported in soils (Darland and Inskeep, 1997). These results suggest that sorption-related non-equilibrium conditions prevailed in the columns. Flow interruptions (24h) were included to further test non-equilibrium conditions in the columns (Figure 4). The flow interruption is a technique that has been used to identify non-equilibrium conditions during the transport of solutes in soils (Brusseau et al., 1989). As shown in Figure 4, a decrease in the concentration of As(V) was observed in the effluent after resuming the flow, indicating additional sorption and, hence, non-equilibrium during transport. This decrease was evidently more pronounced in the columns with the highest pore water velocity (0.78 and 3.75 cm h^{-1}) although a small decrease was also measured in the columns performed at the lowest pore water velocity (0.36 cm h^{-1}) which suggest that they were likely also under non-equilibrium conditions. On the basis of flow interruption-mediated effects it is not possible to differentiate between physical (transport-related) or chemical (sorption-related) non-equilibrium. Because the Br^- breakthrough curves were symmetrical and well described by CDE model, physical non-

equilibrium was ruled out. Thus changes in the outflow concentrations due to flow interruption are likely indicative of chemical non-equilibrium since there is enough time for As(V) to adsorb onto the adsorbant.

3.4 Effect of initial concentration on the transport and retention of As(V)

The effect of the inlet concentration on the efficiency of HA-Goe-coated sand to remove As(V) was investigated by injecting at the same pore water velocity (3.75 cm h^{-1}) two different concentrations of As(V) (1 and 4.6 mg L^{-1}). These concentrations were selected as they are representative of highly contaminated sites. The injection of a solution of higher concentration translated into a much earlier breakthrough of As(V) (Figure 5). The rapid elution of As(V) can be attributed to saturation of sorption sites. If the WHO limit of 10 µg L^{-1} is considered as the guideline for remediation, about 30 PV (low concentration) and 8 PV (high concentration) of contaminated water were filtered before the concentration in the outflow solution surpassed the standard (Figure 5). This number of PVs (30 and 8) are found between 12 to 14 mg As g^{-1} of goethite in the column for low and high As concentrations, *i.e.* about 40% and 45% of the batch adsorption capacity for the HA-Goe-coated sand.

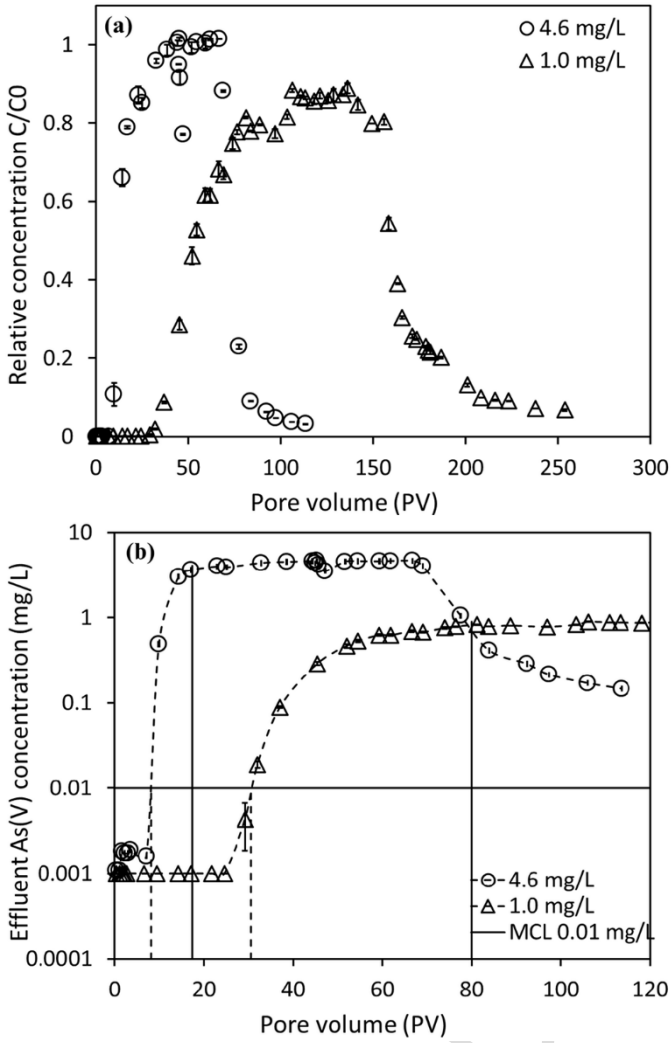

Figure 5 Breakthrough curves for As(V) expressed in relative concentrations (a) and effluent concentration (semi-log plot) (b), at two inlet As(V) concentrations (1 and 4.6 mg L^{-1}) injected at 3.75 cm h^{-1} pore water velocity. The solid horizontal line indicates the maximum concentration limit (MCL) for As in drinking water, the dotted and solid vertical lines is the number of PVs to reach the MCL and the As sorption maximum of the substrate determined in batch.

3.5 Modelling reactive transport of As(V) in columns

To further test the LEA and to validate the reactive transport of As(V), the breakthrough data was modelled with the CDE model in HYDRUS-1D version 4.16. Assuming local equilibrium-governed adsorption and using the Langmuir parameters (b and K_L) from HA-Goe-coated sand (Table 1) from the batch experiments, the transport of a sorbing solute *e.g.* As(V) can be described by:

$$(1 + \frac{\rho}{\theta} \cdot \left[\frac{b \cdot KL}{(1 + KL \cdot c)^2}\right]) \cdot \frac{\delta c}{\delta t} = D\frac{\delta^2 c}{\delta x^2} - v\frac{\delta c}{\delta x} \qquad \text{Eq. 2}$$

where c is the concentration of As(V) adsorbed on equilibrium sites (mg L^{-1}), ρ is the media bulk density (g cm^{-3}), θ is the porosity of saturated media, D is the hydrodynamic dispersion coefficient (cm^2 h^{-1}), *v* the linear water velocity (cm h^{-1}), *t* is the time (h), and *x* the depth (cm). The linear water velocity (*v)* is related to the Darcy's flux (*q*) through the porosity of the saturated media ($q = v \cdot \theta$). The parameters *q*, θ, λ, *b, K_L* are required for HYDRUS-1D input to model the breakthrough data using the equilibrium nonlinear solute transport model. The solute transport boundary conditions selected for modelling the breakthrough data were: flux concentration at the inlet and zero concentration gradient at the outlet.

This nonlinear sorption model with local equilibrium assumption (NLE model) parameterized with batch sorption parameters (*b* and K_L) failed to predict As(V) breakthrough curves from any of the columns with step injections of 4.6 4.9 mg As L^{-1} (Figure 6). The chemical equilibrium model overestimated the breakthrough time. The reason behind this deviation has been ascribed either by the overestimation of retardation with the equilibrium batch adsorption parameters and/or the inability of the solute to reach equilibrium with the adsorbant during the transport through the sand (Seuntjens et al., 2001). It was observed that under flow conditions, only about 50% of the HA-Goe sorption sites were occupied and, hence, the early breakthrough can be due to the by-pass of the As(V)-containing water. Moreover, the nonlinear equilibrium model was also unable to predict the gradual increase in the concentration of As(V) in the effluent (*i.e.* sigmoidal shape of breakthrough curve). The asymmetrical shape of breakthrough curves are better described by non-equilibrium models (Pang et al., 2002). Considering all indications for non-equilibrium sorption, the two-site non-equilibrium transport model was explored to model the breakthrough data. The two-site model considers that the exchange sites are divided into type 1 sites (S_1) that are in equilibrium with the solution phase and type 2 sites (S_2) on which sorption is considered to be time-dependent. In case that sorption is described by the Langmuir equation (Eq. 1), the transport equation for the two-site model is (Šimůnek and van Genuchten, 2008):

$$(1 + \frac{f \cdot \rho}{\theta} \cdot \left[\frac{b \cdot KL}{(1 + KL \cdot c)^2}\right]) \cdot \frac{\delta c}{\delta t} = D\frac{\delta^2 c}{\delta x^2} - v\frac{\delta c}{\delta x} - \frac{\alpha \cdot \rho}{\theta} \cdot [(1 - f) \cdot \frac{b \cdot KL \cdot c}{1 + KL \cdot c} - S_2] \qquad \text{Eq. 3}$$

where *f* is the fraction of equilibrium sites (-), α is the first-order kinetic rate coefficient (h^{-1}), and S_2 the solid phase concentration at site 2 (mg kg^{-1}). The input parameters *q*, θ, λ, *b, K_L, f* and *α* are required for HYDRUS-1D to model the data with the nonlinear non-equilibrium model (NLNE).

461

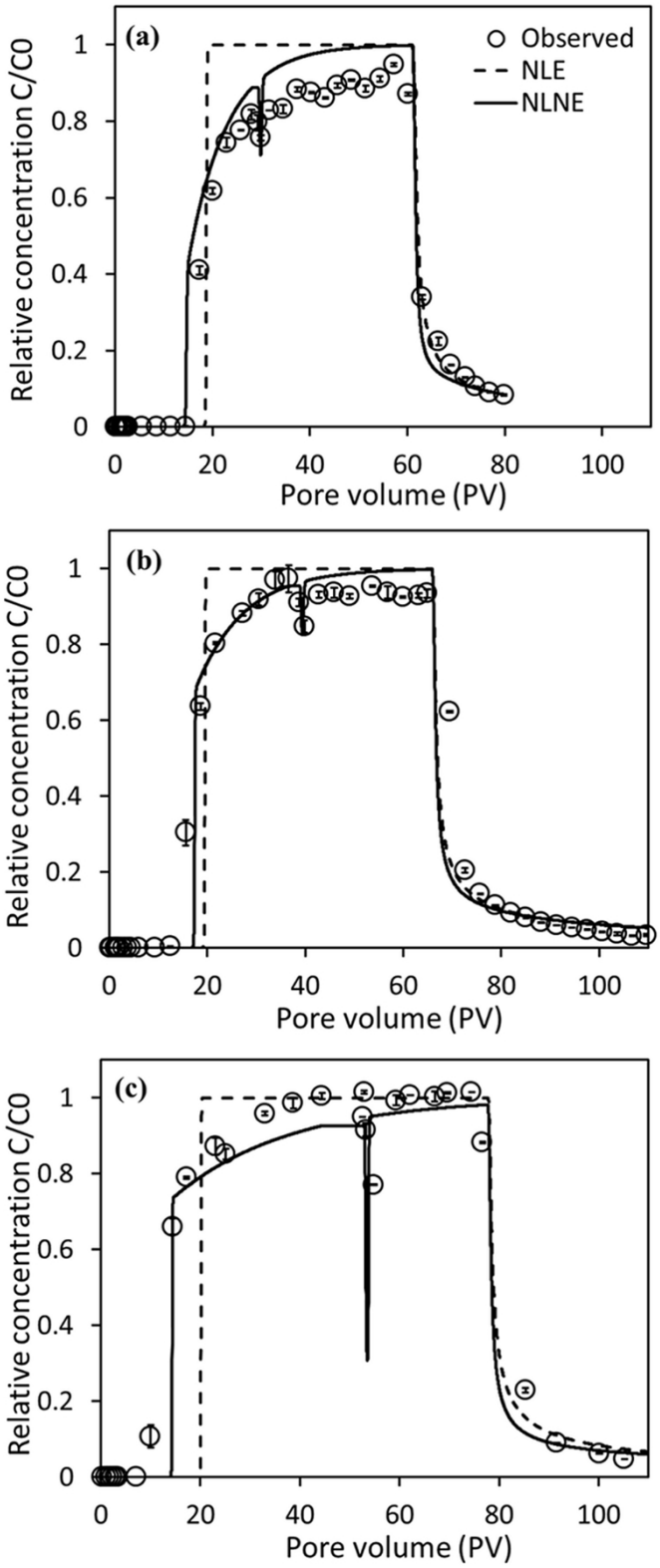

462

463

464 Figure 6 Observed and modelled breakthrough curves for As(V) in columns containing HA-
465 Goe-coated sand at three pore water velocities 0.36 cm h^{-1} (a), 0.78 cm h^{-1} (b) and 3.75 cm h^{-1}
466 (c) and high As(V) inlet concentration. NLE: nonlinear equilibrium model; NLNE: nonlinear

non-equilibrium model. The change in concentration at pore volumes 30 (a), 38 (b) and 47 (c) due to 24-h flow interruption.

For the equilibrium sites the batch equilibrium adsorption parameters were used, whereas the kinetic parameters (*f* and α) were obtained with the inverse solution of HYDRUS-1D by fitting the model to the breakthrough data. As shown in Figure 6, the addition of the kinetic parameters allowed for a better match of the predicted breakthrough curves to the observed data, resulting also in RMSE values of C/C0 that ranged from 0.031 0.038. The values of α increased with increasing pore water velocity (Table 3), which is consistent with previous work (Maraqa, 2001). This kinetic-rate constant describes the sorption/desorption of As(V) in time and is not expected to vary with pore water velocity if the non-equilibrium conditions are mainly due to sorption (chemical non-equilibrium) (Tsang and Lo, 2006). Hence, this finding suggests that physical processes (*i.e.* diffusion) may have also contributed the transport of As(V) in the columns.

Table 3 Chemical non-equilibrium transport parameters derived from the two-site model with standard error in brackets. Errors are based on fitting duplicate columns individually, *i.e.* n=2.

Pore water velocity cm h^{-1}	α h^{-1}	*f*	R^2
0.36	0.004 (0.0001)	0.33 (0.009)	0.988
0.78	0.007 (0.0014)	0.60 (0.028)	0.957
3.75	0.013 (0.0002)	0.53(0.001)	0.967

The velocities used in this study are comparable to those used in previous reported work where the transport of As was described by non-equilibrium models. The groundwater velocities in the field range widely. Typical groundwater velocities are < 1 m $year^{-1}$, equivalent to pore water velocities of 2.5 m $year^{-1}$ or 0.025 cm h^{-1} in which case equilibrium processes can be considered. The transport of As at groundwater velocities of 0.1 10 cm day^{-1} (pore water velocities 0.02 1 cm h^{-1}) was simulated using the empirical parameters (α and *f*) obtained from fitting the columns at 0.36 cm h^{-1}. The model predicted that for the highest velocity (10 cm d^{-1}), only 14 mg As g Goe^{-1} can be adsorbed before exceeding the concentration limit of 10 µg L^{-1} in the effluent water. In contrast, at the lower velocities the equivalent tipping point was close to that determined by batch equilibrium adsorption (about 30 mg As g^{-1} HA-Goe). This indicates that for high flow rates, safety factors should be considered to account for non-equilibrium conditions that can diminish the adsorption efficiency of the adsorbant.

This study was limited to investigate the removal of As(V) from spiked water in packed columns. It is speculated that the challenges to adopt the technology in the field are related to non-homogenous deposition of the particles, the effect of competing ions (*e.g.* phosphates) that can interfere in the adsorption reaction and the longevity of the reactive barrier upon conditions that trigger the reductive dissolution of iron oxides. Furthermore, the release of humic acids (used as coating) from the goethite colloids is also a plausible scenario that may affect the efficiency of remediation through mobilization of metal cations (*e.g.* Zn, Cu) that were adsorbed onto the humic acids. All of the above mentioned factors require further study prior the application of this technology in the field.

4. Conclusions

The results from batch and column experiments showed that HA-Goe colloids can effectively remove As(V) from contaminated water. This study showed that coagulation and deposition of the HA-Goe within the sand matrix (non-colloidal Goe) only marginally affected the adsorption of As and thus deposited HA-Goe were able to remove similar amounts of As(V) compared to the aggregated HA-Goe colloids alone in suspension. Because of the conditions of pH and ionic strength in contaminated groundwater, it is expected that colloids will aggregate and sediment soon after injection. Therefore, the fact that a very high As(V) adsorption capacity was measured (30 mg As g^{-1} HA-Goe), indicates that this is a promising material for remediation of contaminated sites. The relevance of this finding is that more certainty was gained that aggregation and sedimentation processes may not affect the adsorption properties of colloids in field applications.

The experimental breakthrough curves showed that the transport of As(V) exhibited nonlinear and rate-limited reaction. The one dimensional transport model based on LEA failed to correctly describe the breakthrough data and therefore the non-equilibrium model was more appropriate to explain the transport of As(V) in the columns. Because the fitted kinetic rate coefficient was small at the low pore water velocity and large at higher pore water velocities it is likely that the non-equilibrium conditions were related to both diffusion and sorption kinetics. For a successful prediction of As removal in subsurface environments the reactive transport model should include conservative safety factors to account for kinetic-rate expressions and preferential flow paths.

Acknowledgments

530 This work was supported by H2020 EU project “Reground” Grant Agreement N° 641768.
531 www.reground-project.eu/ We thank Dr. Beate Krok (University of Duisburg-Essen,
532 Germany) for providing the stock suspension of goethite colloids.

533 **References**

534 Antelo, J., Arce, F., Fiol, S., 2015. Arsenate and phosphate adsorption on ferrihydrite
535 nanoparticles. Synergetic interaction with calcium ions. Chem. Geol. 410, 53-62.

536 Antelo, J., Avena, M., Fiol, S., López, R., Arce, F., 2005. Effects of pH and ionic strength on
537 the adsorption of phosphate and arsenate at the goethite–water interface. J. Colloid Interface
538 Sci. 285(2), 476-486.

539 Aredes, S., Klein, B., Pawlik, M., 2012. The removal of arsenic from water using natural iron
540 oxide minerals. J. Clean. Prod. 29-30, 208-213.

541 Ayotte, J.D., Gronberg, J.M., Apodaca, L.E., 2011. Trace elements and radon in groundwater
542 across the United States, 1992-2003, U.S. Geological Survey Scientific Investigations Report
543 2011-5059. p. 115.

544 Benjamin, M.M., Sletten, R.S., Bailey, R.P., Bennett, T., 1996. Sorption and filtration of
545 metals using iron-oxide-coated sand. Water Res. 30(11), 2609-2620.

546 Bollyn, J., Nijsen, M., Baken, S., Joye, I., Waegeneers, N., Cornelis, G., Smolders, E., 2016.
547 Polyphosphates and fulvates enhance environmental stability of PO4-bearing colloidal iron
548 oxyhydroxides. J. Agric. Food Chem. 64(45), 8465-8473.

549 Brusseau, M.L., Rao, P.S.C., Jessup, R.E., Davidson, J.M., 1989. Flow interruption: A
550 method for investigating sorption nonequilibrium. J. Contam. Hydrol. 4(3), 223-240.

551 Christian, P., Von der Kammer, F., Baalousha, M., Hofmann, T., 2008. Nanoparticles:
552 structure, properties, preparation and behaviour in environmental media. Ecotoxicology
553 17(5), 326-343.

554 Cundy, A.B., Hopkinson, L., Whitby, R.L.D., 2008. Use of iron-based technologies in
555 contaminated land and groundwater remediation: A review. Sci. Tot. Environ. 400(1–3), 42-
556 51.

557 Darland, J.E., Inskeep, W.P., 1997. Effects of pore water velocity on the transport of arsenate.
558 Environ. Sci. Technol. 31(3), 704-709.

559 Dixit, S., Hering, J.G., 2003. Comparison of arsenic (V) and arsenic (III) sorption onto iron
560 oxide minerals: implications for arsenic mobility. Environ. Sci. Technol. 37(18), 4182-4189.

561 Downs, R.T., Hall-Wallace, M., 2003. The American mineralogist crystal structure database.
562 Am. Mineral. 88, 247-250.

563 Fritzsche, A., Rennert, T., Totsche, K.U., 2011. Arsenic strongly associates with ferrihydrite
564 colloids formed in a soil effluent. Environ. Pollut. 159(5), 1398-1405.

565 Giménez, J., Martínez, M., de Pablo, J., Rovira, M., Duro, L., 2007. Arsenic sorption onto
566 natural hematite, magnetite, and goethite. J. Hazard. Mater. 141(3), 575-580.

567 Hotze, E.M., Phenrat, T., Lowry, G.V., 2010. Nanoparticle aggregation: challenges to
568 understanding transport and reactivity in the environment J. Environ. Qual. 39(6), 1909-1924.

569 Karn, B., Kuiken, T., Otto, M., 2009. Nanotechnology and *in situ* remediation: A review of
570 the benefits and potential risks. Environ. Health Perspect. 117(12), 1823-1831.

571 Kleber, M., Eusterhues, K., Keiluweit, M., Mikutta, C., Mikutta, R., Nico, P.S., 2015.
572 Mineral–organic associations: formation, properties, and relevance in soil environments.
573 Adv. Agron. 130, 1-140.

574 Kosmulski, M., 2009. pH-dependent surface charging and points of zero charge. IV. Update
575 and new approach. J. Colloid Interface Sci. 337(2), 439-448.

576 Mähler, J., Persson, I., 2013. Rapid adsorption of arsenic from aqueous solution by
577 ferrihydrite-coated sand and granular ferric hydroxide. Appl. Geochem. 37, 179-189.

578 Mamindy-Pajany, Y., Hurel, C., Marmier, N., Roméo, M., 2011. Arsenic (V) adsorption from
579 aqueous solution onto goethite, hematite, magnetite and zero-valent iron: Effects of pH,
580 concentration and reversibility. Desalination 281, 93-99.

581 Maraqa, M.A., 2001. Prediction of mass-transfer coefficient for solute transport in porous
582 media. J. Contam. Hydrol. 50(1), 1-19.

583 Meckenstock, R., Bosch, J., 2014. Method for the degradation of pollutants in water and/or
584 soil. U.S. Patent 8921091 B2. Issued Dec 30, 2014.

585 Mohan, D., Pittman, C.U., 2007. Arsenic removal from water/wastewater using adsorbents—
586 A critical review. J. Hazard. Mater. 142(1–2), 1-53.

587 Murcott, S., 2012. Arsenic contamination in the world. IWA publishing, London.

588 Otero-Fariña, A., Fiol, S., Arce, F., Antelo, J., 2017. Effects of natural organic matter on the
589 binding of arsenate and copper onto goethite. Chem. Geol. 459, 119-128.

590 Pang, L., Close, M., Schneider, D., Stanton, G., 2002. Effect of pore-water velocity on
591 chemical nonequilibrium transport of Cd, Zn, and Pb in alluvial gravel columns. J. Contam.
592 Hydrol. 57(3–4), 241-258.

593 Philippe, A., Schaumann, G.E., 2014. Interactions of dissolved organic matter with natural
594 and engineered inorganic colloids: a review. Environ. Sci. Technol. 48(16), 8946-8962.

595 Saldaña-Robles, A., Saldaña-Robles, N., Saldaña-Robles, A.L., Damian-Ascencio, C.,
596 Rangel-Hernández, V.H., Guerra-Sanchez, R., 2017. Arsenic removal from aqueous solutions
597 and the impact of humic and fulvic acids. J. Clean. Prod. 159, 425-431.

598 Scheidegger, A., Borkovec, M., Sticher, H., 1993. Coating of silica sand with goethite:
599 preparation and analytical identification. Geoderma 58(1–2), 43-65.

600 Seuntjens, P., Tirez, K., Šimůnek, J., van Genuchten, M.T., Cornelis, C., Geuzens, P., 2001.
601 Aging effects on cadmium transport in undisturbed contaminated sandy soil columns. J.
602 Environ. Qual. 30(3), 1040-1050.

603 Šimůnek, J., van Genuchten, M.T., 2008. Modeling nonequilibrium flow and transport
604 processes using HYDRUS Vadose Zone J. 7(2), 782-797.

Šimůnek, J., van Genuchten, M.T., Šejna, M., Toride, N., Leij, F.J., 1999. The STANMOD computer software for evaluating solute transport in porous media using analytical solutions of convection-dispersion equation. Versions 1.0 and 2.0, , International Ground Water Modeling Center, Colorado School of Mines. U.S. Salinity Laboratory, U.S.D.A. Riverside California.

Smedley, P.L., Kinniburgh, D.G., 2002. A review of the source, behaviour and distribution of arsenic in natural waters. Appl. Geochem. 17(5), 517-568.

Socrates, G., 2004. Infrared and rama characteristic group frequencies: tables and charts, 3 ed. John Wiley & Sons Ltd., Chichester.

Tosco, T., Petrangeli Papini, M., Cruz Viggi, C., Sethi, R., 2014. Nanoscale zerovalent iron particles for groundwater remediation: a review. J. Clean. Prod. 77, 10-21.

Tsang, D.C.W., Lo, I.M.C., 2006. Influence of pore-water velocity on transport behavior of cadmium: equilibrium versus nonequilibrium. J. Hazard Toxic Radioact. Waste 10(3), 162-170.

Weng, L., Van Riemsdijk, W.H., Hiemstra, T., 2009. Effects of fulvic and humic acids on arsenate adsorption to goethite: experiments and modeling. Environ. Sci. Technol. 43(19), 7198-7204.

Weng, L.P., Koopal, L.K., Hiemstra, T., Meeussen, J.C.L., Van Riemsdijk, W.H., 2005. Interactions of calcium and fulvic acid at the goethite-water interface. Geochim. Cosmochim. Acta 69(2), 325-339.

WHO, 2011. Guidelines for drinking-water quality, 4th ed., Geneva, World Health Organization. www.who.int/water_sanitation_health/publications/2011/dwq_guidelines/en/ (accessed 06.10.2017).

Williams, L.E., Barnett, M.O., Kramer, T.A., Melville, J.G., 2003. Adsorption and transport of arsenic(V) in experimental subsurface systems. J. Environ. Qual. 32(3), 841-850.

Wu, P.-Y., Jia, Y., Jiang, Y.-P., Zhang, Q.-Y., Zhou, S.-S., Fang, F., Peng, D.-Y., 2014. Enhanced arsenate removal performance of nanostructured goethite with high content of surface hydroxyl groups. J. Environ. Chem. Eng. 2(4), 2312-2320.

Zhang, H., Selim, H.M., 2006. Modeling the Transport and Retention of Arsenic (V) in Soils Soil Sci. Soc. Am. J. 70(5), 1677-1687.

Efficient removal of arsenate from oxic contaminated water by colloidal humic acid-coated goethite: batch and column experiments

Daniela Montalvo[*1], Ruth Vanderschueren[1], Andreas Fritzsche[2], Rainer U. Meckenstock[3], and Erik Smolders[1]

[1]Division of Soil and Water Management, KU Leuven, Kasteelpark Arenberg, Heverlee, Belgium

[2] Institut für Geowissenschaften, Friedrich-Schiller-Universität Jena, D-07749 Jena, Germany

[3] Biofilm Centre, University Duisburg-Essen, 45141 Essen, Germany

[*]Corresponding author E-mail address: daniela.montalvogrijalva@kuleuven.be

Highlights

- Humic acid-coated goethite (HA-Goe) can effectively remediate As(V) polluted water.
- Main advantage of HA-Goe is their high As(V) adsorption capacity (30 mg As g^{-1}).
- HA-Goe colloids retain their sorption capacities after coagulation in sand.
- Non-equilibrium transport model predicts As(V) transport in flow-through conditions.